Numerical simulation for the heat transfer of a helical double-pipe vertical evaporator
Proceedings of European Congress of Chemical Engineering (ECCE-6)
Copenhagen, 16-20 September 2007

Numerical simulation for the heat transfer of a helical double-pipe vertical evaporator

D. Colorado-Garrido,[a] E. Santoyo-Castelazo[a], J. A.Hernandez[b], O. García-Valladares[c], D. Juarez-Romero[b], J. Siqueiros[b]

[a] *Posgrado en Ingeniería y Ciencias Aplicadas, Universidad Autónoma del Estado de Morelos, Av. Universidad 1001. Col. Chamilpa, C.P. 62209 Cuernavaca, Morelos, México*
[b] *Centro de Investigación en Ingeniería y Ciencia Aplicadas, Universidad Autónoma del Estado de Morelos, Av. Universidad 1001. Col. Chamilpa, C.P. 62209 Cuernavaca, Morelos, México.*
[c]*Centro de Investigación en Energía (CIE), Universidad Nacional Autónoma de México(UNAM), Privada Xochicalco S/N, Tenixco, 62580, Morelos México*

Abstract

A predictive model is developed to describe the heat transfer and fluid dynamic behavior of a helical double-pipe vertical evaporator used in a waste energy recovery heat transformer by water purification process. The evaporator uses water as working fluid connected in countercurrent. The heat transfer by conduction in the internal tube wall is considered; in addition the change of phase is carried out into the internal tube. The dynamic model considers equations of continuity, momentum and energy in each flow. A model by Artificial Neural Network is proposed for the thermodynamics properties required in each point of the grid in which the domain is discretized. The results of this model are compared with the experimental data in steady state, obtained good simulations of the evaporator in the process (errors Q < 1.0%). Dynamic model will evaluate and determine the principals operation variables that affect the evaporator with the main objective to optimize and control the system.

Keywords: step by step, heat transfer, helical tube, implicit method, water purification.

1. Introduction

The efficient use of the energy resources and the water contamination are two important problems at present. The heat transformer is a system that consists of a thermodynamic device capable of producing useful heat at a thermal level superior to the one in the source (Santoyo-Gutierrez et al., 1999). The advantage of this heat transformer is that it may be used in any other system that requires a temperature greater than the one provided by the source. Therefore, in this context, a number of works report that it is possible to integrate the heat transformer to a water purification process (Holland et al., 1990, Santoyo-Gutierrez et al., 1999). The water purification system here proposed is a simple distillation process where impure water is heated to

obtain vapor which is immediately condensed. The condenser releases heat and pure water. This integration of both systems enables to increase the temperature of the impure water system, and thus to obtain pure water and useful heat. In the energy cycle of an absorption heat transformer there are four main components: absorber (AB), evaporator (EV), generator (or desorber) (GE), and condenser (CO). In this type of energy cycle (absorption heat transformer), the Coefficient of Performance (COP) is a very important variable for determining their performance (Rivera Gomez Franco, 1996). This COP (eq. 1) is defined as the ratio of heat delivered in the absorber divided by the heat load supplied to the generator plus evaporator.

$$COP = \frac{Q_{AB}}{Q_{EV} + Q_{GE}} \tag{1}$$

Different thermodynamic models have been reported for heat transformers, Rivera Gomez Franco, (1996) developed a thermodynamic model for heat transformer using different working fluids. Siqueiros et al., (2007) and Romero et al., (2007) report increase in COP for heat transformer using a thermodynamic model. These models follow some assumptions, for example:

- The entire system is in thermodynamic equilibrium,
- The analysis is carried out under steady-state conditions,
- Heat losses and pressure drops in the tubing and the components are considered negligible (AB, GE, EV and CO),
- A heat supply is delivered by industrial waste heat,

Helical coiled tubes are extensively used in steam generators, refrigerators, nuclear reactors and chemical plants, etc., due to their practical importance of high efficiency heat transfer, compactness in structure, ease of manufacture and arrangement (Zhao at al, 2003).

Consequently, with the purpose to determine the COP of an absorption heat transformer integrated to a water purifications system, this work presents a dynamic model to describe the heat transfer and fluid dynamic behavior inside of a helical double-pipe vertical evaporator (EV). The applications of this work are related with the optimization and control of the absorption heat transformer system.

2. Experimental data

Experimental data by Santoyo-Castelazo and Siqueiros, (2007), consist of different COP values (*without* energy recycling and *with* energy recycling (Siqueiros and Romero, 2007)). This data were obtained from a water purification system integrated to a single stage heat transformer. The experimental system was operated at different concentrations of the LiBr+H_2O mixture, different temperatures in AB, GE, EV, CO and different pressures in AB and GE. In addition of the experimental data of each component, the steady state is taken into account for each initial concentration used in

the process. From this database only the experimental data of the evaporator (EV) is considered.

The evaporator has a design of a helical double-pipe. The whole system was constructed by stainless steel tubes and was well isolated by foam insulation. Table 1 describes the dimensions of the helical evaporator. In the internal pipe, working fluid flow (water), which changes from liquid phase to vapour phase, takes into account the heat from the heating water (annulus).

Table 1: Dimensions of the helical double pipe evaporator

	Internal pipe (mm)	External pipe (mm)
External diameter	19.2	32.7
Internal diameter	16.9	29.1
Helical diameter	400	400
Turns	4.5	4.5
Length	5655	5655
Height	310	310

Figure 1 shows the inlet and outlet flows in the evaporator. The working fluid in the evaporator inlet (E2), which comes from the condenser (CO), undergoes a change of phase, which is transformed in outlet vapor (S2). This outlet vapor in the evaporator goes to the absorber (AB), which is now converted in inlet working fluid in the absorber to continued the energy cycle (Siqueiros and Romero 2007).

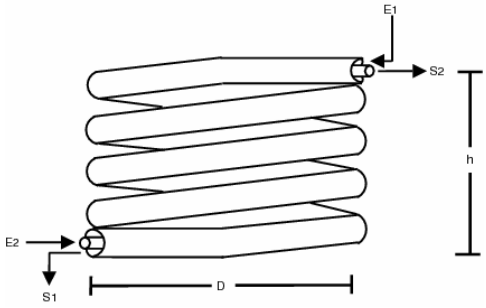

Figure 1: Helical double-pipe evaporator experimental

The experimental information is as follows: for internal pipe, the system mass flow rate was not implemented only mass flow rate is registered for the annulus pipe. A vacuum gauge Bourdon type was employed to measure the pressure in the inlet vapor from the absorber. The assumption that the outlet pressure from the evaporator is equal to the registered at the inlet vapour from the absorber was considered. In order to monitor the bulk temperature, four thermocouples T-type (copper-constantan) were installed at the inlet and outlet flows (in positions E1, S1, E2 and S2) of evaporator.

2.1 Experimental uncertainty analysis

In the present work, the quantities measured directly were, flow rate, pressure and bulk temperature.

The flowmeter had an accuracy of ±3%. The internal flow rate was calculated in base of an external balance of evaporator, because the evaporator does not have the necessary instrumentation to measure it. The vacuum gauge uncertainty was estimated to be less than 0.5% of full scale. The measurements of thermocouples had a precision ± 1ºC.

3. Mathematical formulation of two phase flow.

In this section describe the mathematical formulation over a control volume. A control volume is a finite volume that delimits a physical space corresponding to a partial or global zones of a thermal unit (García-Valladares, 2000), for this case, the helical evaporator. A control volume is show in Figure 2, where "i" and "i+1" represents the inlet and outlet sections, respectively.

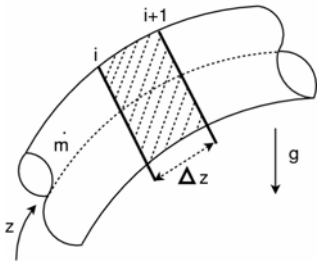

Figure 2: flow inside a helical control volume

Taking into account the characteristic helical coils, the governing equations have been integrated assuming the following (García-Valladares, 2007):

- Fluid: water,
- One-dimensional flow: p(z, t), h(z, t), T(z, t), etc.,
- Non-participant radiations medium and negligible radiant heat exchanger between surfaces,
- Axial heat conduction inside the fluid is neglected,
- Constant internal and coiled diameters and uniform roughness surface.

The semi-integrated governing equations (continuity, momentum, energy and entropy) over control volume were presented by García-Valladares (2004). For each control volume, a set of algebraic equations is obtained by a discretization of the governing equations. The transient terms of the governing equations are discretized using the following approximation $\partial\phi/\partial t \cong \left(\phi - \phi^{o}\right)\big/\Delta t$, where ϕ represents a generic dependent variable (ϕ= h, p, T, etc.); superscript "o" indicates the value of the previous instant. The average of the different variables has been estimated by the arithmetic mean between their values at the inlet and outlet sections, that is: $\widetilde{\phi}_i \cong \overline{\phi}_i \equiv \left(\phi_i + \phi_{i+1}\right)/2$

Based on the numerical approaches indicated above, the governing equations can be discretized to obtain the value of the dependent variables (mass flow rate, pressure and enthalpy) at the output section of each control volume.

The mass flow rate is obtained from the discretized *continuity equation*,

$$\dot{m}_{i+1} = \dot{m}_i - \frac{A\Delta z}{\Delta t}\left(\overline{\rho}_{tp} - \overline{\rho}^{o}_{tp}\right) \tag{2}$$

Where the two-phase flow density is obtained from: $\rho_{tp} = \varepsilon_g \rho_g + \left(1-\varepsilon_g\right)\rho_l$

In terms of the mass flow rate, gas and liquid velocities are calculated as follows,

$$v_g = \left[\frac{\dot{m}\, x_g}{\rho_g \varepsilon_g A}\right];\ v_l = \left[\frac{\dot{m}\left(1-x_g\right)}{\rho_l\left(1-\varepsilon_g\right)A}\right]$$

The discretized *momentum equation* is solved for the outlet pressure

$$p_{i+1} = p_i - \frac{\Delta z}{A}\left(\Phi \frac{f}{4}\frac{\overline{\dot{m}^2}}{2\overline{\rho}_{tp}A^2}P + \overline{\rho}_{tp}Ag\sin\theta + \frac{\left[\dot{m}\left(x_g v_g + \left(1-x_g\right)v_l\right)\right]_i^{i+1}}{\Delta z} + \frac{\overline{\dot{m}} - \overline{\dot{m}}^{o}}{\Delta t}\right) \tag{3}$$

The subscript and superscript in the brackets indicate $\left[X\right]_i^{i+1} = X_{i+1} - X_i$ the difference between the quality (X) at the outlet section and the inlet section. Evaluated momentum equation (3) considers pressure drop in the flow of the internal pipe.

From the energy equation and the continuity equation, the following equation is obtained for the output enthalpy:

$$h_{i+1} = \frac{2\dot{q}P\Delta z - \dot{m}_{i+1}\,a + \dot{m}_i\,b + \dfrac{A\Delta z}{\Delta t}c}{\dot{m}_{i+1} + \dot{m}_i + \dfrac{\left(\tilde{\varepsilon}^{o}_{g}\tilde{\rho}^{o}_{g} + \left(1-\tilde{\varepsilon}^{o}_{g}\right)\tilde{\rho}^{o}_{l}\right)A\Delta z}{\Delta t}} \tag{4}$$

Where:

$$a = \left(x_g v_g + \left(1-x_g\right)v_l\right)_{i+1}^2 + g\sin\theta\Delta z - h_i$$

$$b = \left(x_g v_g + \left(1-x_g\right)v_l\right)_{i}^2 - g\sin\theta\Delta z + h_i$$

$$c = 2\left(\overline{p}_i - \overline{p}_i^{o}\right) - \tilde{\rho}^{o}_{tp}\left(h_i - 2\overline{h}_i^{o}\right) - \left(\overline{\rho v_i^2} - \overline{\rho}^{o} v_i^{o^2}\right)$$

These equations need the values of thermodynamic properties. Temperature, mass fraction, density, etc. are calculated from correlations presented in the next section *Calculation of thermodynamic properties in two phase flow for water***.**

The one-dimensional model requires the knowledge of the two-phase flow structure, which is evaluated by means of void fraction ε_g. The evaluation of the stress is performed by means of a friction factor *f*. This factor is defined from the expression: $\tau = \Phi\left(f/4\right)\left(G^2/2\rho\right)$ where Φ is the two-phase factor multiple (García-

Valladares, 2007). The inertial, centrifugal and gravity forces are embroiled in the calculation of friction factor for the helical coil. A heat transfer through the helical wall and fluid temperature are related by the convective heat transfer coefficient α, which is defined as:

$$\alpha = \frac{q_{wall}}{\left(T_{wall} - T_{fluid}\right)} \tag{5}$$

In the same way, the calculation of convective heat transfer involves previously mentioned effects.

In the internal pipe of helical evaporator, different regions are presented during the evaporation. The differentiations between the three principal regions are given by the enthalpy, pressure and vapour quality, then following these equations:

$$c = 0.4788 + \left[0.8658\left(p\right)\right] \tag{6}$$

$$d = \frac{2}{\left(1 + \exp\left(-2c\right)\right)} - 1 \tag{7}$$

$$\begin{pmatrix} h_l \\ h_g \end{pmatrix} = d \begin{pmatrix} 1.3663 \\ 0.0682 \end{pmatrix} + \begin{pmatrix} -0.1949 \\ 0.9393 \end{pmatrix} \tag{8}$$

Where p is pressure (bar), c and d are constant, and h_l and h_g are the saturation liquid and vapor enthalpy (kJ/kg). The result for this formulation is incorporated into the following criterion (García-Valladares, 2000).

- Liquid region: when $h(p) < h_l(p)$, then $x_g = 0$
- Two-phase region: when $h_l(p) \leq h(p) \leq h_g(p)$, then $0 < x_g < 1$.
- Vapor region: when $h(p) > h_g$, then $x_g = 1$.

Where $h_l(p)$ and $h_g(p)$ represent the saturation liquid and gas enthalpy for a given pressure p.

3.1. Calculation thermodynamic properties in two phase flow for water.

Table generated for the NIST/ASME Steam properties Database (NIST), were determined. With this database, an artificial neural network was developed to calculate thermodynamic properties. This is based on the limits of operations of the helical evaporator. These models were developed in order to offer an easy, direct and precise tool for the calculation of thermodynamics properties. The equations that this work proposes to calculate the thermodynamic properties for water two phase flow are:

$$c = b1 + \left[Wi1 \begin{pmatrix} p \\ h \end{pmatrix} \right] \tag{9}$$

$$\varphi = \left(Wo2\right) d + b2 \tag{10}$$

Where pressure and enthalpy are independent variables; **d** is calculated by eq. (7) and φ is the thermodynamic property to calculate. The result of these matrix operations is the thermodynamic properties in evaporation flow or annulus section, depending to Wi1, Wo2, b1 and b2 values (see Appendix).

3.2 Heat conduction in the internal and external tube wall

The physical space that separates the flows, tube wall, is treated assuming the following hypotheses: one-dimensional transient temperature distribution and negligible heat exchanger by radiation. The energy balance used to describe heat transfer in the wall is obtained (see figure 3):

$$\left(\tilde{\dot{q}}_{ns}P_{ns} - \tilde{\dot{q}}_{nn}P_{nn}\right)\Delta z + \left(\tilde{\dot{q}}_{nw} - \tilde{\dot{q}}_{ne}\right)A = m\frac{\partial \tilde{h}}{\partial t} \tag{11}$$

Where $\tilde{\dot{q}}_{ns}$ and $\tilde{\dot{q}}_{nn}$ are evaluated using the respective convective heat transfer coefficient in each zone, and the conductive heat transfer fluxes are evaluated from the Fourier law, which is: $\tilde{\dot{q}}_{ne} = -\lambda_{ne}\left(\partial T/\partial z\right)_{ne}$ and $\tilde{\dot{q}}_{nw} = -\lambda_{nw}\left(\partial T/\partial z\right)_{nw}$.

The heat transfer in external tube wall was not considered. Therefore, the heat conduction in the insulation element and the natural convection with the environment are neglected.

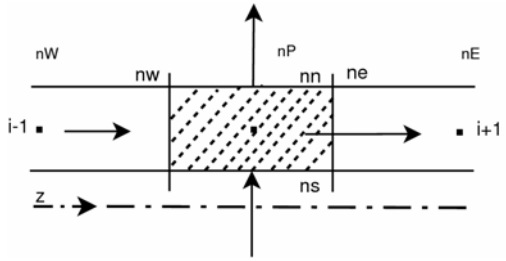

Figure 3: Heat fluxes in a control volume of a wall

4. Evaluation of empirical coefficients

A comparison of different empirical correlations presented in the literature (Pabhanjan, D.G. et al, 2003, Wongwises S. et al. 2006, Rennie T.J., 2006, García A. et al., 2005, Cui W. et al, 2006, Guo et al., 2001, Ko, 2006 and Zhao et al., 2003) was realized in order to select the following ones to obtain the best results.

4.1 *Single-phase region, liquid and vapor in internal pipe.*

The friction factor is evaluated from the following expression proposed by Schmidt (Guo et al., 2001) also suggested a correlation for the laminar region in curved pipes:

$$\frac{f_c}{f_s} = \left[1 + 0.14 \left(\frac{d}{D} \right)^{0.97} \mathrm{Re} \right]^i \tag{12}$$

Where $i = 1 - 0.644 \left(d/D \right)^{0.312}$ and $f_s = 64/\mathrm{Re}$. In the case of turbulent region the friction factor is evaluated with the equation proposed by Ito:

$$f_c = 1.216 \, \mathrm{Re}^{-0.25} + 0.116 \left(\frac{d}{D} \right)^{0.5} \tag{13}$$

Guo at al., (2001) recommended this equation as the standard formula for the turbulent region. The convective heat transfer coefficient is calculated using the Nusselt from the proposed by Churchill (Ko, 2006), correlation for the laminar region in helical coiled tubes is:

$$Nu = \left[\left(\frac{48}{11} + \frac{51/11}{\left(1 + \frac{1342}{\mathrm{Pr} \, He^2} \right)^2} \right)^3 + 1.816 \left(\frac{He}{1 + \frac{1.15}{\mathrm{Pr}}} \right)^{3/2} \right]^{1/3} \tag{14}$$

The Nusselt number to evaluate turbulent region, the proposed by Sebas and McLaughlin (Zhao et al., 2003) is used:

$$Nu = 0.023 \, \mathrm{Re}^{0.8} \, \mathrm{Pr}^{0.4} \left[\mathrm{Re} \left(d/D \right)^2 \right]^{0.05} \tag{15}$$

4.2 *Two phase flow region, in internal pipe.*

The scope of this model does not consider different flow regimen of evaporation phenomenon, for example sub-cooled boiling and post-dryout. The void fraction is evaluated according to a semi-empirical relations proposed by Rouhani et al, (1970).

$$\varepsilon_g = \frac{x_g}{\rho_g} \left[\left(\left[1 + 0.12 \left(1 - x_g \right) \right] \left(\frac{x_g}{\rho_g} + \frac{1 - x_g}{\rho_l} \right) \right) + \frac{1.18 \left(1 - x_g \right) \left[g \sigma_l \left(\rho_l - \rho_g \right) \right]^{0.25}}{G \rho_l^{0.5}} \right]^{-1} \tag{16}$$

In two phase flow, the friction factor is calculated from a correlation by Churchill, (1977) using correction factor (two-phase frictional multiplier) according to (Friedel, 1979). The convective heat transfer coefficient is calculated from a correlation by Kozeki's (Zhao at al., 2003). This correlation involved Martinelli parameter.

$$\frac{h_{tp}}{h_l} = 2.5 \left(\frac{1}{Xtt} \right)^{0.75} \tag{17}$$

The convective heat transfer coefficient for single-phase is evaluated by the correlation proposed by Sebas and McLaughlin (Zhao et al., 2003), described previously in equation (15).

4.3 *Annulus.*

The factor friction and heat transfer coefficient in the annulus section are evaluated with the hydraulic diameter using the single-phase flow correlations.

5. Numerical solution

The main objective is to determine the heat transfer and flow behavior through the helical evaporator. The discretized equations have been coupled using a fully implicit step by step method in the flow direction. From the known values at the inlet section, the variables values at the outlet of each control volume are iteratively obtained. This solution (outlet values) is the inlet values for the next control volume. The procedure is carried out until the end of the helical evaporator is reached.

The conditions of differentiation between regions are mentioned in the *Mathematical formulation of two phase flow* section and the equations (6), (7) and (8) the control volume where the transition occurs is detected. The transition criterion used for internal pipe is that once the control volume is detected, where the transition between regions takes place, the beginning of this transition is associated with the control volume exit. The criterion is important to calculate the appropriated empirical coefficients for each zone.

In each control volume, mass, momentum and energy discretized equations (algebraic equations) given certain initial and boundary conditions, are solved by an iterative method for to obtain the output solution. This outlet solution is used to initial condition of next control volume moving forward step by step in the flow direction. Inside each control volume, the convergence was verified using the following criterion (eq. 18):

$$\left(1-\left|\frac{\phi_{i+1}^{*}-\phi_{i}}{\Delta\phi}\right|\right)<\delta \tag{18}$$

Here, ϕ is the mass flow rate, pressure and enthalpy. The superindex * represents the values at the previous iteration. The referent values $\Delta\phi$ is evaluated in each control volume: $\phi_{i+1}-\phi_i$. When this value tends to be zero, is substituted by ϕ_i.

The heat conduction in the wall was discretized in accordance by García Valladares, (2004). The set of heat conduction discretized equations is solved using the tri-diagonal matrix algorithm.

The numerical global model to describe the heat transfer and dynamic flow behavior is as follows: The dominium of helical evaporator is discretized in a fixed number of control volumes; one dimensional flow was adopted in internal and annulus flow; in the wall, solid element to separate the flows, a displaced mesh was used; initial conditions in the flows are necessary. The algorithm follows next sequence:

1.-Initial conditions of flows were specified, mass flow rate, pressure and temperature. If flow quality is known, this data is used.
2.-Suppose a temperatures distribution in the wall.

3.-The flow in internal pipe is solved. In this section two-phase flow is present.
4.-The flow in the annulus is solved, in this barometric pressure of the experiment are calculated.
5.-re-calculate the temperature distribution in wall with the temperature distribution in the flows and heat transfer coefficients using a tri-diagonal matrix algorithm.

These steps repeat themselves up to verify a strict convergence criterion (eq. 18). The steady-state is a particular form for this model, where it is not considered the temporary derivative in the equations.

6. Numerical results

Experimental conditions (Test A, see Table 2) are used to determine the influence of the number to control volume over numerical results obtained for the outlet temperature, pressure and enthalpy in internal pipe and annulus. Figure 4 shows results independence of spatial mesh obtained with $n_z \geq 500$ control volumes.

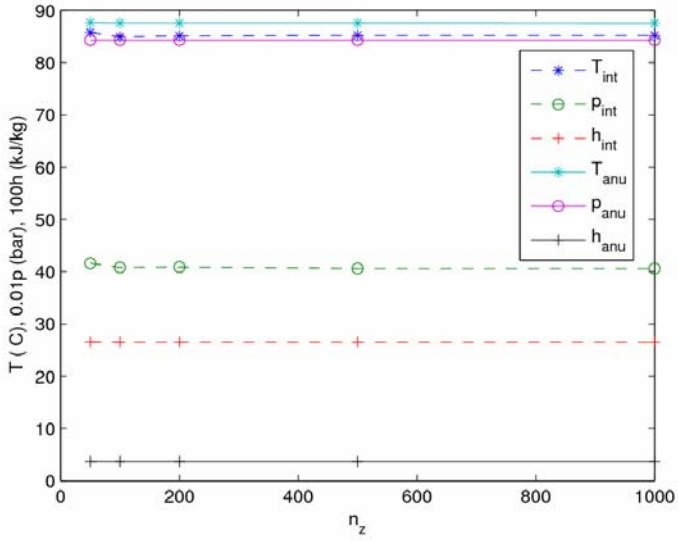

Figure 4: Outlet temperature, pressure and enthalpy obtained for different number of control volume in internal pipe and annulus. The convergence criterion was $\delta = 10^{-5}$

The model in steady-state, with 500 control volume, $\Delta z = 0.0113$ m and convergence criterion $\delta = 10^{-5}$, is compared with experimental data by (Santoyo-Castelazo, 2005 and 2007). This model used initial experimental values in steady-state of the input flows. Table 2 shows the results compared outlet values of flows. Tests A, B and C are experimental operation condition for (Santoyo-Castelazo, 2005). Tests D and E are results of the experimental modifications over absorber with aim to incrementing COP of heat transformer. Tests F, G, H and I are experimental conditions to operating helical evaporator while recycling heat from auxiliary condenser (Siqueiros at al, 2007). An important characteristic of the model is that *no parameter was adjusted* to describe the heat transfer in evaporator.

Table 2: Experimental database of helical evaporator vs. numerical results

	Internal pipe				Annulus		
	Exp		Sim.		Exp.	Sim.	
Test	T_{outlet} (ºC)	p_{outlet} (bar)	T_{outlet} (ºC)	p_{outlet} (bar)	T_{outlet} (ºC)	T_{outlet} (ºC)	p_{outlet} (bar)
A	85.27±1	0.4080±0.01	85.20	0.4059	87.00±1	87.56	0.8429
B	84.75±1	0.3911±0.01	76.86	0.3799	86.57±1	86.19	0.8422
C	78.85±1	0.3741±0.01	72.92	0.3260	79.60±1	82.66	0.8430
D	83.01±1	0.2726±0.01	86.94	0.2759	84.00±1	84.49	0.8422
E	83.26±1	0.3064±0.01	87.46	0.3105	84.76±1	85.30	0.8422
F	81.45±1	0.3741±0.01	73.62	0.2982	80.57±1	83.25	0.8427
G	85.21±1	0.3697±0.01	76.95	0.3337	82.13±1	84.38	0.8426
H	79.97±1	0.3741±0.01	77.80	0.3182	80.92±1	83.60	0.8426
I	80.99±1	0.3741±0.01	72.92	0.2904	80.82±1	83.30	0.8423

Figures 5, 6 and 7 show the simulated distribution of temperature and pressure while a change of phase takes place in the internal pipe and the experimental data for the tests A, D and G. These figures denote that the model proposed represents the temperature and pressure behavior across the pipe in a reliable way.

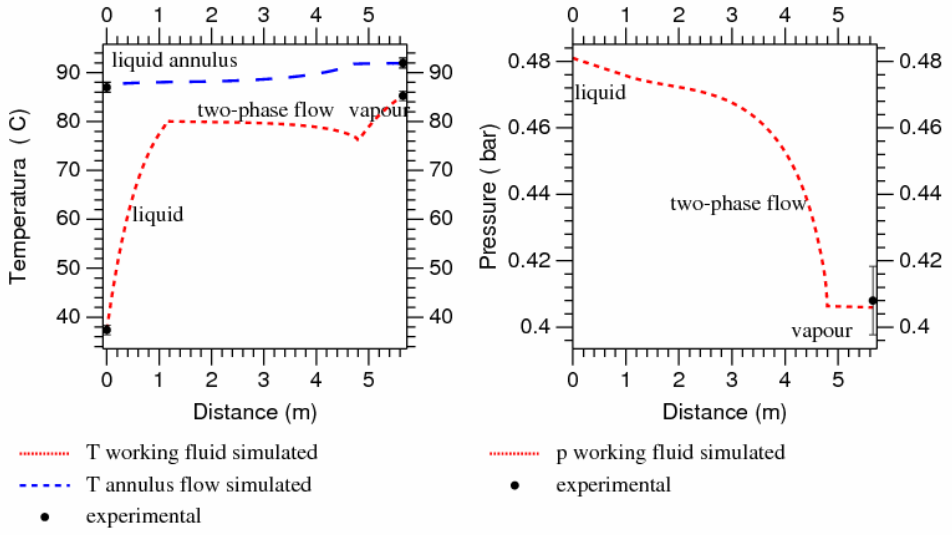

Figure 5: Simulated vs. experimental data by test A (see Table2) in steady-state.

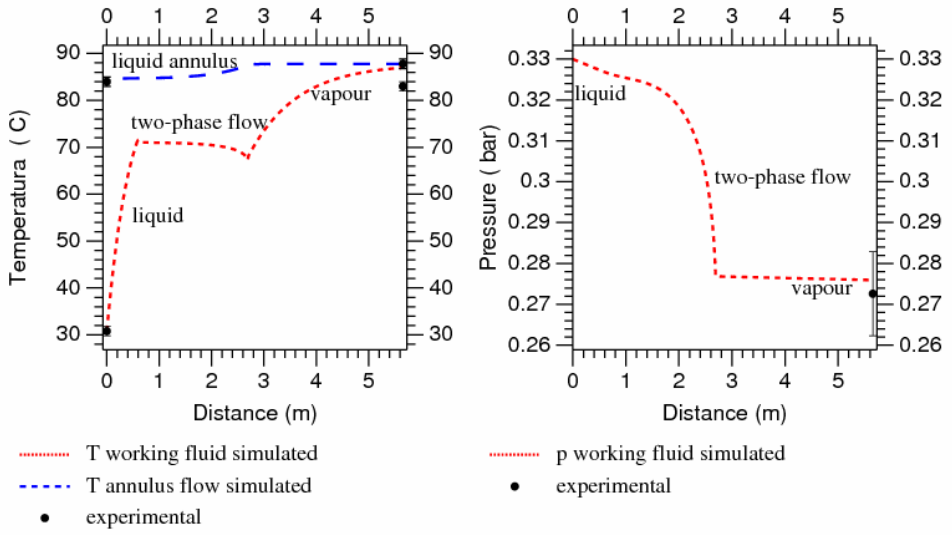

Figure 6: Simulated vs. experimental data by test D (see Table2) in steady-state

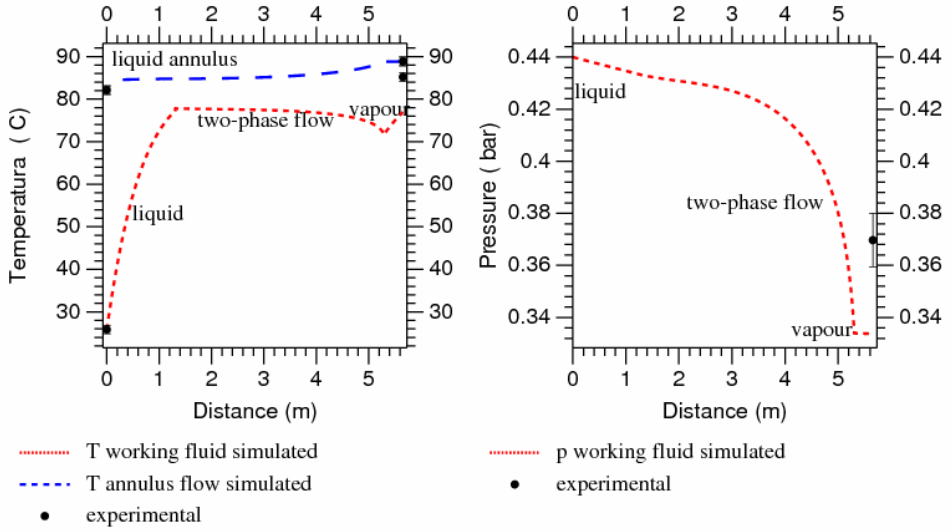

Figure 7: Simulated vs. experimental data by test G (see Table2) in steady-state

Experimental data presents variations in the operating conditions of helical double pipe evaporator from experimental data by Santoyo-Castelazo and Siqueiros (2007). The same working fluid (water) and helical geometry was used. Variations in outlet pressure, inlet and outlet temperature and mass flux rate are reported. The heat flux calculated for these 9 tests subestimate the experimental results with a discrepancy smaller than that 1.0 %, (see Table 3) with a mean deviation of 0.45%. Moreover the model is based on the applications of physical laws it is possible to extrapolate other operating conditions with a minor error (1.0%).

Table 3: Comparison of the heat flux (Q internal flow) between simulation and experimental results by Santoyo-Castelazo

Test	exp. Q (kW)	sim. Q (kW)	Error %
A	3.24	3.24	0.00
B	2.91	2.89	-0.68
C	2.82	2.80	-0.70
D	2.16	2.16	0.00
E	1.91	1.91	0.00
F	3.60	3.58	-0.55
G	3.31	3.28	-0.90
H	3.49	3.49	0.00
I	3.84	3.81	-0.78

6. Conclusions

A numerical model of heat transfer and fluid dynamic behavior of a helical double-pipe evaporator has been developed by means of a transient one-dimensional analysis of the flows together with a detail analysis of the heat conduction in the internal wall. The empirical coefficients used in the model to evaluate the shear stress, heat flux and two phase structure had been used in technical literature for helical systems. The selected coefficients have been compared with experimental results of helical evaporator.

Finite volume formulations of the governing equations in two phase flow were used. The model implements an implicit step by step numerical scheme for the working fluid and fluid in the annulus and implicit central difference numerical scheme in the internal wall. The outlet of control volume is solved based by iterative method in a segregated manner until convergence is reached, given certain initial conditions.

Comparisons of experimental and simulated data in steady-state for 9 tests show a mean deviation of 0.45% for the heat flux. Further studies will try to adapt this dynamic model to general thermodynamic for heat transfer technologies, for future design, optimization, control and on-line estimation of COP.

Acknowledgements

This study has been supported by the “Consejo Nacional de Ciencia y Tecnología“ CONACYT-México (Project SEP-2004-C01-48024) and PROMEP-UAMOR-PTC-158.

Nomenclature

A Cross area section (m^2)
AB Absorber

CO Condenser
COP Coefficient of performance
Cp Specific heat at constant pressure (J kg^{-1} $ºC^{-1}$)
D Helical diameter (m)
d Internal diameter (m)
Dn Dean number ($Dn = \mathrm{Re}\left(d/D\right)^{1/2}$)
e Specific energy (h + $v^2/2$ + gz sinθ) (J kg^{-1})
EV Evaporator
f Friction factor
g Acceleration due to gravity (m s^{-2})
GE Generator
He Helical number ($He = Dn \Big/ \left[1+\left(b/2\pi\left(d/2\right)\right)^2\right]^{1/2}$)
G Mass velocity (kg m^{-2} s^{-1})
h Enthalpy (J kg^{-1})
L Reference length (m)
$\dot{m}$ Mass flow rate (kg s^{-1})
m mass (kg)
n_z Number of control volumes
Nu Nusselt number ($Nu = \alpha d \big/ \lambda$)
p Pressure (bar)
P Perimeter (m)
Pr Prandtl number ($\mathrm{Pr} = Cp\mu/\lambda$)
$\dot{q}$ Heat flux per unit area (W m^{-2})
Q Heat flux rate (W)
Re Reynolds number (Re = Gd/μ)
t Time (s)
T Temperature (^oC)
CV Control volume
v Velocity (m s^{-1})
Xtt Martinelli parameter $\left(\left(\frac{1-x_g}{x_g}\right)^{0.9}\left(\frac{\rho_g}{\rho_l}\right)^{0.5}\left(\frac{\mu_g}{\mu_l}\right)^{0.1}\right)$
x_g Vapor mass fraction
z Axial coordinate

Greek letters

θ Angle (rad)
ρ Density (kg m^{-3})
δ Convergence criterion
σ Superficial tension (N m^{-1})
Φ Two-phase frictional multiplier

α	Heat transfer coefficient (W m^{-2} $^oC^{-1}$)
τ	Shear stress (Pa)
λ	Thermal conductivity (W m^{-1} $^oC^{-1}$)
μ	Dynamic viscosity (Pa s)
ξ	Absolute roughness (m)
$\in_g$	Void fraction
Δt	Temporal discretization step (s)
Δz	Axial discretization step (m)

Subscript:

Ab	Absorber
Anu	Annulus
c	Coiled
s	Straight
exp	Experimental
sim	Simulate
Int	Internal pipe
g	Vapor
tp	Two-phase flow
l	Liquid

superscripts

^{o}	Previous instant
*	Previous iteration

References

Churchill, S.W., (1977), Frictional equations spans all fluid flow regimes, *Chem Engng*, **84**:91-2

Cui W., Li L., Xin M., Jen T., Chen Q, Lian Q., (2006), A heat transfer correlation of flow boiling in micro-finned helically coiled tube, *International Heat and Mass Transfer*, revised form 16 February 2006.

Friedel L., (1979), Improved friction pressure drop correlation for horizontal and vertical two-phase pipe flow, *European Two-Phase Flow Group Meeting*, Ispra, Italy, Paper E2.

García-Valladares O., Pérez-Segarra C.D and Rigola J., (2004), Numerical simulation of double-pipe condensers and evaporators, *Int. J. Refrigeration*, **27**, 656-670

García-Valladares O, (2000), Simulación numérica y validación experimental de evaporadores, condensadores y tubos capilares. Integración en sistemas de refrigeración por compresión, PhD thesis, Departamento de maquinas y motores térmicos, Universidad politécnica de Cataluña, Terrassa, España.

García A., Vicente P.G. and Viedma A, (2005), Experimental study of heat transfer enhancement with wire coil inserts in laminar-transition-turbulent regimes at different Prandt numbers, *International Heat and Mass Transfer,* **48**, 4640-4651.

García-Valladares O., (2007), Numerical simulation and experimental validation of coiled adiabatic capillary tubes, *Applied Thermal Engineering*, **27**, 1062-1071.

Guo L., Feng Z. and Chen X., (2001), An experimental investigation of the frictional pressure drop of steam-water two-phase flow in helical coils, *Int. J. Heat and Mass Transfer*, **44**, 2601-2610.

Holland F.A., (1999), Fundamentos y aspectos económicos de las bombas de calor, manual sobre tecnología de bombas de calor, Program of cooperation and investigation between Instituto de Investigaciones Eléctricas, Cuernavaca, México and Salford University, UK.

Ko T.H., (2006), Thermodynamic analysis of optimal curvature ratio for fully developed laminar forced convection in a helical coiled tube with uniform heat flux, *Int. J. of Thermal Sciences*, **45**, 729-737.

Morales Gómez L.I., (2005), Estudio experimental sobre un sistema portátil de purificación de agua integrado a un transformador térmico, Master thesis, Facultad de Ciencias Químicas e Ingeniería, Universidad Autónoma del Estado de Morelos, Cuernavaca, Morelos, México.

NIST Standard Reference Database 10, *NIST/ASME Steam properties Database*, Version 2.11, USA

Prabhanjan D.G., Rennie, T.J. and Raghavan V., (2003), Natural convection heat transfer from helical coiled tubes, *International Journal of Thermal Sciences*, **43**, 359-365.

Rennie T.J. and Raghavan V.G.S., Effects of fluid thermal properties on the heat transfer characteristics in double –pipe helical heat exchanger, *International Journal of Thermal Sciencies,* accepted 20 February 2006.

Rivera Gomez Franco W, (1996), Heat transformer technology and steam generation, PhD thesis, University of Salford. UK.

Romero R.J., Siqueiros J, Huicochea A., (2007), Increase of COP for heat transformer in water purification systems. Part II –Without increasing heat source temperature, *Applied Thermal Engineering*, **27**, 1054-1061.

Rouhani Z., Axelsson E., (1970), Calculation of volume void fraction in the subcooled and quality region, *Int. J. Heat Mass Transfer*, **13**:383-93

Santoyo-Castelazo E., (2005), Modificaciones para incrementar la eficiencia de un sistema de purificación de agua integrado a un transformador térmico y pruebas preliminares, Engineering thesis, Facultad de Ciencias Químicas e Ingeniería, Universidad Autónoma del Estado de Morelos, Cuernavaca, Morelos.

Santoyo-Castelazo E. and Siqueiros J., (2007), Estudio experimental de un transformador térmico acoplado a un transformador térmico, Memorias del XXVIII Encuentro Nacional de la AMIDIQ, TER-21, 4072-4085.

Santoyo-Gutierrez S., Siqueiros J., Heard C.L., Santoyo E., Holland F. A., (1999), An experimental integrated absorption heat puma effluent purification system. Part I: operating on water/lithium bromide solutions, *Applied Thermal Engineering*, **19,** 461-475.

Siqueiros J., and Romero R.J., (2007), Increase of COP for heat transformer in water purification systems. Part I – Increasing heat source temperature, *Applied Thermal Engineering*, **27**, 1042-1053.

Wongwises S., Polsongkram M., (2006), Evaporation heat transfer and pressure drop of HFC-134a in a helically coiled concentric tube-in-tube heat exchanger, *Int. J. Heat and Mass Transfer,* **49**, 658-670.

Yi J., Liu Z. and Wang J., (2003), Heat transfer characteristics of the evaporator section using small helical coiled pipes in a looped heat pipe, *Applied Thermal Engineering*, **23,** 89-99.

Zhao L., Guo L., Bai B., Hou Y. and Zhang X., (2003), Convective boiling heat transfer and two-phase flow characteristics inside a small horizontal helically coiled tubing once-through steam generator, *Int. J. Heat and Mass Transfer*, **46**, 4779-4788.

Appendix

Weight and bias necessary to calculated thermodynamic properties

Table 4: Annulus (single-phase liquid) [a]

φ	IW	LW	B_1	b_2
T (^oC)	(0.0002 -0.7233)	-1.3951	0.5899	0.8225
ρ ($kg\ m^{-3}$)	(0.0007 -1.2576)	0.0485	1.3695	0.9692
μ ($\mu Pa\ s$)	(-0.0015 -2.7186)	-0.0062	2.7329	0.9346
λ ($mW\ m^{-1}\ ^oC^{-1}$)	(-0.0043 -2.0033)	-0.0709	0.9781	0.9386
Cp ($kJ\ Kg^{-1}\ ^oC^{-1}$)	(-0.0015 -2.7186)	-0.0062	2.7329	0.9346

[a] *operation range 0.8010 <=p(bar)<=0.8350; 230<=h(kJ/kg)<=370*

Table 5: Liquid single-phase in internal pipe [b]

φ	IW	LW	b_1	b_2
T (^oC)	(0.0000 -0.3829)	-2.6151	0.2439	0.6355
ρ ($kg\ m^{-3}$)	(0.0010 -1.2085)	0.0394	1.3173	0.9692
μ ($\mu Pa\ s$)	$\begin{pmatrix} 0.0005 & 1.2492 \\ -15.9078 & 7.6605 \end{pmatrix}$	(-3.3488 0.0004)	$\begin{pmatrix} 0.6715 \\ 0.2925 \end{pmatrix}$	3.6064
λ ($mW\ m^{-1}\ ^oC^{-1}$)	$\begin{pmatrix} 0.0528 & -5.7363 \\ 0.0002 & -1.2297 \end{pmatrix}$	(0.0002 0.1790)	$\begin{pmatrix} 3.1177 \\ 0.0852 \end{pmatrix}$	0.8530
Cp ($KJ\ kg^{-1}\ ^oC^{-1}$)	$\begin{pmatrix} -0.0026 & 0.9977 \\ -0.0084 & -2.8128 \end{pmatrix}$	(0.0489 1.5351)	$\begin{pmatrix} -2.2347 \\ -2.7442 \end{pmatrix}$	2.5754

[b] *operation range 0.15<= p(bar)<=0.45; 100<= h(kJ/kg)<=329.09*

Table 6: Vapour [c]

φ	IW	LW	b_1	b_2
T (^oC)	(-0.0032 -2.9573)	-2.0396	2.6735	0.6022
ρ ($kg\ m^{-3}$)	$\begin{pmatrix} -2.3730 & 5.2489 \\ 1.3538 & -8.3876 \end{pmatrix}$	(-0.2615 6.0484)	$\begin{pmatrix} -2.7962 \\ 3.8842 \end{pmatrix}$	6.6556
μ ($\mu Pa\ s$)	(0.0027 4.0957)	0.8267	-3.8682	0.9045
λ ($mW\ m^{-1}\ ^oC^{-1}$)	(0.0149 5.1470)	0.7799	-5.0146	0.9971
Cp ($kJ\ kg^{-1}\ ^oC^{-1}$)	$\begin{pmatrix} -5.0458 & -0.5985 \\ 0.7145 & -17.1194 \\ -0.7601 & 32.8878 \end{pmatrix}$	(-0.0045 -0.0229 -1.0453)	$\begin{pmatrix} 4.9109 \\ 15.7141 \\ -25.2677 \end{pmatrix}$	2.0265

[c] *operation range 0.36 <= p(bar)<= 0.45; 2632.3 <= h(kJ/kg)<= 3000*

Table 7: Two-phase flow [d]

φ	IW	LW	b_1	b_2
T (^oC)	$\begin{pmatrix} -1.9054 & -0.0000 \\ -1.9773 & -0.0000 \end{pmatrix}$	$\begin{pmatrix} -0.1392 & -3.3568 \end{pmatrix}$	$\begin{pmatrix} 1.4931 \\ -1.1661 \end{pmatrix}$	-2.3803
ρ_l (kg/m^3)	$\begin{pmatrix} -1.4818 & 0.0000 \\ -2.1054 & -0.0000 \end{pmatrix}$	$\begin{pmatrix} 0.0102 & 0.0318 \end{pmatrix}$	$\begin{pmatrix} 1.1543 \\ -0.4329 \end{pmatrix}$	1.0139
ρ_v (kg/m^3)	$\begin{pmatrix} 0.3315 & 0.0000 \end{pmatrix}$	(3.3175)	-0.0066	0.0445
μ_l (μPa s)	$\begin{pmatrix} -1.1197 & 0.0000 \\ 4.5164 & 0.0000 \end{pmatrix}$	$\begin{pmatrix} 0.5309 & -1.3354 \end{pmatrix}$	$\begin{pmatrix} 1.1514 \\ -0.5970 \end{pmatrix}$	2.3637
μ_v (μPa s)	$\begin{pmatrix} -1.7588 & 0.0000 \\ 1.9736 & 0.0000 \end{pmatrix}$	$\begin{pmatrix} 0.0352 & 0.5459 \end{pmatrix}$	$\begin{pmatrix} -1.3757 \\ 1.0279 \end{pmatrix}$	0.4199
λ_l ($mW\ m^{-1}\ ^oC^{-1}$)	$\begin{pmatrix} 1.8421 & 0.0000 \\ -2.8151 & -0.0000 \end{pmatrix}$	$\begin{pmatrix} 0.0142 & -1.4718 \end{pmatrix}$	$\begin{pmatrix} -1.1175 \\ -1.7431 \end{pmatrix}$	-0.4818
λ_v ($mW\ m^{-1}\ ^oC^{-1}$)	$\begin{pmatrix} 0.5302 & -0.0000 \\ 3.2038 & 0.0000 \end{pmatrix}$	$\begin{pmatrix} 0.4358 & 0.6355 \end{pmatrix}$	$\begin{pmatrix} 0.4346 \\ 1.3586 \end{pmatrix}$	0.0133
Cp_l ($kJ\ kg^{-1}\ ^oC^{-1}$)	$\begin{pmatrix} 0.623 & 0.0000 \end{pmatrix}$	0.0100	-0.0668	0.9949
Cp_v ($kJ\ kg^{-1}\ ^oC^{-1}$)	$\begin{pmatrix} 0.623 & 0.0000 \end{pmatrix}$	$\begin{pmatrix} 0.0490 & 0.8963 \end{pmatrix}$	$\begin{pmatrix} 0.4515 \\ 2.2103 \end{pmatrix}$	0.0514
X_g	$\begin{pmatrix} -0.0139 & 0.3006 \end{pmatrix}$	3.4359	0.4554	-0.1588
h_{lg} ($KJ\ Kg^{-1}$)	$\begin{pmatrix} 2.2815 & -0.0000 \\ -1.6992 & -0.0000 \end{pmatrix}$	$\begin{pmatrix} -0.0087 & 0.6130 \end{pmatrix}$	$\begin{pmatrix} -1.8617 \\ -1.5456 \end{pmatrix}$	1.5746
σ ($N\ m^{-1}$)	$\begin{pmatrix} -0.6465 & -0.0000 \\ -4.5855 & -0.0002 \end{pmatrix}$	$\begin{pmatrix} -0.2501 & -0.0327 \end{pmatrix}$	$\begin{pmatrix} 0.3667 \\ -0.2818 \end{pmatrix}$	1.1230

[d] *operation range 0.2<= p(bar)<= 0.5; 275.24<= h(kJ/kg)<=2621.9*